Experimental and Theoretical Studies on the Selectivity of GGG Triplets toward One-Electron Oxidation in B-Form DNA

Yasunori Yoshioka,*,† Yasutaka Kitagawa,† Yu Takano,† Kizashi Yamaguchi,*,† Takashi Nakamura,‡ and Isao Saito*,‡,§

Contribution from the Department of Chemistry, Graduate School of Science, Osaka University, Toyonaka, Osaka 560-0043, Japan, Department of Synthetic Chemistry and Biological Chemistry, Faculty of Engineering, Kyoto University, Kyoto 606-8501, Japan, and CREST, Japan Science and Technology Corporation, Chiyoda-ku, Tokyo 102-0081, Japan

Received March 31, 1999

Abstract: The selectivity of 5′-TGGGT-3′ and 5′-CGGGC-3′ sequences toward photoinduced one-electron oxidation was examined experimentally and by ab initio molecular orbital (MO) calculations. It was confirmed experimentally that G_2 of 5′-$TG_1G_2G_3$T-3′ is more reactive than G_1, while for 5′-$CG_1G_2G_3$C-3′ the selectivity is reversed, that is, $G_1 > G_2$. The ab initio MO analyses were performed to elucidate the difference of the selectivities between 5′-TGGGT-3′ and 5′-CGGGC-3′ sequences. For the 5′-TGGG-3′ sequence, the spin densities of $G_1^\bullet$ and $G_2^\bullet$ in neutral radical (5′-$TG_1G_2G_3$-3′)$^\bullet$ have a similar pattern, and the shapes of the corresponding radical orbitals are also very similar. It was concluded that the selectivity is due to the stability of the (5′-$TG_1G_2G_3$-3′)$^\bullet$ neutral radicals; that is, 5′-$TG_1G_2^\bullet G_3$-3′ is more stable in energy than 5′-$TG_1^\bullet G_2G_3$-3′. For the 5′-CGGG-3′ sequence, it was found that the spin density on N1 of $G_1^\bullet$ in neutral radical (5′-$CG_1G_2G_3$-3′)$^\bullet$ is distinguishably different from the corresponding spin density of $G_2^\bullet$, which has a pattern similar to those of $G_1^\bullet$ and $G_2^\bullet$ in 5′-$TG_1G_2G_3$-3′. The radical orbital (SOMO) of $G_1^\bullet$ is delocalized on guanine base and up to the paired cytosine base, while the radical orbital of $G_2^\bullet$ is essentially localized on guanine base. This drastic difference of the electron population in the radical orbitals, caused by the stacking interaction with the 5′-side G of the opposite strand, can explain why G_1 is more reactive than G_2 in the 5′-$CG_1G_2G_3$-3′ sequence.

Introduction

Long-range DNA damage caused by one-electron oxidation of nucleobases has been extensively studied from the viewpoint of mutagenesis and carcinogenesis induced by carcinogenic agents, ionizing radiation, photosensitization with endogenous photosensitizers, and high-intensity laser irradiation.[1−8] Since guanine is the most easily oxidized base among DNA nucleobases,[4,5] guanine radical cation is the initial product of DNA one-electron oxidation in a wide variety of systems.[5−7] The electron-loss center created in DNA duplex by one-electron oxidation ultimately moves to end up at guanine (G) base via hole migration through the DNA π stack. As is well known, 5′-G of 5′-GG-3′ sequences is selectively oxidized in the B-form DNA in reaction systems using a variety of oxidizing agents.[9−17]

* To whom correspondence should be addressed. Y.Y.: phone 06-6850-5406; fax 06-6850-5550; e-mail yyoshi@chem.sci.osaka-u.ac.jp. K.Y.: phone 06-6850-5404; fax 06-6850-5550; e-mail yama@chem.sci.osaka-u.ac.jp. I.S.: phone 075-753-5656; fax 075-753-5676; e-mail saito@sbchem.kyoto-u.ac.jp.

† Osaka University.

‡ Kyoto University.

§ CREST.

(1) (a) Saito, I.; Takayama, M.; Sugiyama, H.; Nakamura, T. In *DNA and RNA Cleavers and Chemotherapy of Cancer and Viral Diseases*; Meunier, B., Ed.; NATO ASI Series; Kluwer Academic Publishers: Dordrecht, The Netherlands, 1996; pp 163−176. (b) Hall, D. B.; Holmin, R. E.; Barton, J. K. *Nature* **1996**, *382*, 731. (c) Arkin, M. R.; Stemp, E. D. E.; Pulver, S. C.; Barton, J. K. *Chem. Biol.* **1997**, *4*, 389. (d) Holmin, R. E. Dandliker, P. J.; Barton, J. K. *Angew. Chem., Int. Ed. Engl.* **1997**, *36*, 2714. (e) Hall, D. B.; Barton, J. K. *J. Am. Chem. Soc.* **1997**, *119*, 5045. (f) Gasper, S. M.; Schuster, G. B. *J. Am. Chem. Soc.* **1997**, *119*, 12762. (g) Hall, D. B.; Kelley, S. O.; Barton, J. K. *Biochemistry* **1998**, *37*, 15933. (h) Kelley, S. O.; Barton, J. K. *Science* **1999**, *283*, 375.

(2) (a) Meggers, E.; Michel-Beyerle, M. E.; Giese, B. *J. Am. Chem. Soc.* **1998**, *120*, 12950. (b) Ratner, M. *Nature* **1998**, *397*, 480.

(3) Saito, I.; Nakamura, T.; Nakatani, K.; Yoshioka, Y.; Yamaguchi, K.; Sugiyama, H. *J. Am. Chem. Soc.* **1998**, *120*, 12686.

(4) Oxidation potentials of nucleobases, see, for example: (a) Seidel, C. A. M.; Shulz, A.; Sauer, H. M. *J. Phys. Chem.* **1996**, *100*, 5541 and references therein. (b) Steenken, S.; Jovanovic, S. V. *J. Am. Chem. Soc.* **1997**, *119*, 617.

(5) For a review, see Burrows, C. J.; Muller, J. G. *Chem. Rev.* **1998**, *98*, 1109.

(6) (a) Candeias, L. P.; Steenken, S. *J. Am. Chem. Soc.* **1992**, *114*, 699. (b) Sevilla, M. D.; D'Arcy, J. B.; Morehouse, K. M.; Engelhardt, M. L. *Photochem. Photobiol.* **1979**, *29*, 37. (c) Graslund, A.; Ehrenberg, A.; Rupprecht, A.; Storm, G. *Photochem. Photobiol.* **1979**, *29*, 245. (d) Meggers, E.; Kusch, D.; Spichty, M.; Wille, U. P.; Giese, B. *Angew. Chem., Int. Ed. Engl.* **1998**, *37*, 460.

(7) Melvin, T.; Botchway, S.; Parker, A. W.; O'Neill, P. *J. Chem. Soc., Chem. Commun.* **1995**, 653.

(8) (a) Cullis, P. M.; McClymoun, J. D.; Symons, M. C. R. *J. Chem. Soc., Faraday Trans.* **1990**, *86*, 591. (b) Breen, A. P.; Murphy, J. A. *Free Radical Biol. Med.* **1995**, *18*, 1033. (c) O'Neill, P.; Fielden, E. M.; *Adv. Radiat. Biol.* **1993**, *17*, 53.

(9) (a) Saito, I.; Takayama, M.; Sugiyama, H.; Nakatani, K.; Tsuchida, A.; Yamamoto, M. *J. Am. Chem. Soc.* **1995**, *117*, 6406. (b) Sugiyama, H.; Saito, I. *J. Am. Chem. Soc.* **1996**, *118*, 7063.

(10) Stemp, E. D. E.; Arkin, M. R.; Barton, J. K. *J. Am. Chem. Soc.* **1997**, *119*, 2921.

(11) Breslin D. T.; Schuster, G. B. *J. Am. Chem. Soc.* **1996**, *118*, 2311. (b) Ly, D.; Kan, Y.; Armitage, B.; Schuster, G. B. *J. Am. Chem. Soc.* **1996**, *118*, 8747. (c) Armitage B.; Ly, D.; Koch, T.; Frydenlund, H.; Ørum, H.; Batz, H. G.; Schuster, G. B. *Proc. Natl. Acad. Sci. U.S.A.* **1997**, *94*, 12320.

(12) (a) Ito, K.; Inoue, S.; Yamamoto, K.; Kawanishi, S. *J. Biol. Chem.* **1993**, *268*, 13221. (b) Kino, K.; Saito, I.; Sugiyama, H. *J. Am. Chem. Soc.* **1998**, *120*, 7373.

(13) (a) Nakatani, K.; Dohno, C.; Nakamura, T.; Saito, I. *Tetrahedron Lett.* **1998**, *39*, 2779. (b) Nakatani, K.; Fujisawa, K.; Dohno, C.; Nakamura, T.; Saito, I. *Tetrahedron Lett.* **1998**, *39*, 5995.

(14) Ito, K.; Kawanishi, S. *Biochemistry* **1997**, *36*, 1774.

(15) Muller, J. G.; Hickerson, R. P.; Perez, R. J.; Burrows, C. J. *J. Am. Chem. Soc.* **1997**, *119*, 1501.

(16) Shih, H.-C.; Tnag, N.; Burrows, C. J.; Rokita, S. E. *J. Am. Chem. Soc.* **1998**, *120*, 3284.

10.1021/ja991032t CCC: $18.00
Published on Web 09/10/1999

Precise mapping of such GG-containing hot spots in one-electron oxidation of B-form DNA has also been accomplished.[3] These GG doublets are often used as a probe for the terminus in the long-range hole migration.[1−3,11]

It was also demonstrated that 5′-GGG-3′ triplets act as a more effective trap in hole migration than 5′-GG-3′ doublets.[2a,3,9] For example, Kawanishi and co-workers have observed that the central G's of 5′-AGGGA-3′, 5′-AGGGT-3′, and 5′-TGGGT-3′ sequences are selectively damaged under photosensitization with riboflavin and pterin.[12a,14] Spassky and co-workers have also shown that direct two-photon excitation of B-form DNA with a high-energy laser pulse leads to damage of central G in a variety of 5′-GGG-3′ triplets.[17b]

On the other hand, it was reported by Barton and co-workers that the duplexes containing 5′-CGGGC-3′ sequence are primarily cleaved at the 5′-side G using Rh and Ru metallointercalators.[1b−d] This is in conflict with our previous finding that the central G is selectively damaged in the 5′-TGGGT-3′ sequence in the photooxidation sensitized by naphthalimide derivatives and ribflavin.[9a] Recently, Giese and co-workers[2a] and Barton and co-workers[1g] also reported, similarly, that a selective damage at the central G is observed on 5′-TGGGT-3′ sequences.

Several years ago, we demonstrated for the first time both experimentally and by ab initio molecular orbital (MO) calculations that 5′-G's of 5′-GG-3′ doublets in B-form DNA are the most easily oxidized due to the GG stacks and can act as thermodynamic sinks in hole migration across the DNA π stack.[1a,9] We also demonstrated that the highest occupied molecular orbital (HOMO) of a GG stack is essentially high in energy and concentrated on the 5′-G.[9b] In a previous paper, we demonstrated a precise mapping of G-rich hot spots such as 5′-TXGYT-3′ experimentally and by ab initio MO calculations.[3] A linear correlation between the relative susceptibility toward one-electron oxidation versus the calculated ionization potentials was obtained. It was also shown that the theoretical ionization potentials provide a simple way to predict the relative reactivity toward one-electron oxidation. The GGG sequence has the lowest ionization potential (IP) of 6.34 eV at the HF/6-31G* level among other G-containing -XGY- sequences,[3] indicating that the GGG triplet is most easily oxidized in DNA one-electron oxidation. It is thus concluded that GG doublets and GGG triplets act as effective traps in long-range hole migration in DNA one-electron oxidation.[2a,3]

Theoretical calculations of DNA bases have been extensive for IPs of monomer nucleobases, stability of nucleobase pair in neutral and radical cation states, and stacking interactions between nucleobases.[9b,18] However, only a few ab initio calculations on stacked nucleobases have been reported.[9b,18d,e] Theoretical analyses for one-electron oxidation of GGG triplets are scarcely found.

In this work, we examined the detailed analyses of the selectivities of 5′-$TG_1G_2G_3T$-3′ and 5′-$CG_1G_2G_3C$-3′ sequences toward photoinduced one-electron oxidation. It was confirmed experimentally that G_2 of 5′-$TG_1G_2G_3T$-3′ is more reactive than G_1, while for 5′-$CG_1G_2G_3C$-3′ the ordering of the selectivity is reversed, that is, $G_1 > G_2$, consistent with previous results.[1,2,9,12,14] In both sequences, the 3′-side G (G_3) was far less reactive than G_1 and G_2. We next performed the ab initio MO analyses to elucidate the reason the selectivity of 5′-$CG_1G_2G_3C$-3′ is different from that of 5′-$TG_1G_2G_3T$-3′.

Experimental Sections

General. Riboflavin (**1**) was purchased from Nacalai Tesque Co. Ltd., and cyano-substituted benzophenone **2** was synthesized as reported previously.[13a] Calf thymus DNA was purchased from Pharmacia Biotech. The oligodeoxynucleotides d(CGTACTCTTGGTTCGGG-CTTGGGTTTCTTTCTT) (33 mer), its complementary strand d(AA-GAAAGAAACCCAAGCC-CGAACCAAGAGTACG) (33 mer), d(CATTCGGGCTTG) (12 mer), and its complementary strand d(CAAGCCCGAATG) (12 mer) were purchased from Greiner Japan Co. Ltd. The oligodeoxynucleotide d(ATGGGTACCCAT) was synthesized on an Applied Biosystems model 392 DNA/RNA synthesizer and purified by HPLC. T_4 kinase was purchased from NIPPON GENE (10 units/μL), and [γ-^{32}P]-ATP (10 mCi/mL) was from Amersham. All aqueous solutions utilized purified water (Millipore, Milli-Q sp UF). Photoirradiation at 366 nm was carried out using a Cosmo BIO CSF-20AF transilluminator. Photoirradiation at 312 nm was carried out using a Vilber Lourmat TFX-20M transilluminator. A Gibco BRL model S2 sequencing gel electrophoresis apparatus was used for polyacrylamide gel electrophoresis (PAGE). The gels were analyzed by autoradiography with a Bio-Rad Model GS-700 imaging densitometer and Bio-Rad Molecular Analyst software (version 2.1). CD spectra were recorded on a Jasco J-720 spectropolarimeter.

Preparation of 5′-^{32}P-End-Labeled ODN. The oligonucleotide 33 mer (400 pmol-strand) was 5′-end-labeled by phosphorylation with 4 μL of [γ-^{32}P]-ATP and 4 μL of T_4 polynucleotide kinase using standard procedures.[19] The 5′-end-labeled oligonucleotides were recovered by ethanol precipitation, further purified by 15% preparative nondenaturing gel electrophoresis, and isolated by the crush-and-soak method.[20]

Cleavage^{32}P-End-Labeled ODNs by Photoirradiation in the Presence of Photosensitizer. 5′-^{32}P-End-labeled ODN 33 mer was hybridized to the complementary strand (2.5 μM, strand concentration) in 10 mM sodium cacodylate buffer, pH = 7.0, without salts such as NaCl. Hybridization was achieved by heating the sample at 90 °C for 5 min and slowly cooling to room temperature. The 5′-^{32}P-end-labeled ODN duplex (2.0×10^5 cpm) containing a photosensitizer, and calf thymus DNA (10 μM, base concentration) was irradiated with a transilluminator at 4 °c for 40 min. After irradiation, all reaction mixtures were ethanol-precipitated with the addition of 10 μL of 3 M sodium acetate and 800 μL of ethanol. The precipitated DNA was washed with 100 μL of 80% cold ethanol and dried in vacuo. The dried DNA was dissolved in 50 μL of water or 10% piperidine (v/v), heated at 90 °C for 20 min, evaporated by vacuum rotary evaporation to dryness, and resuspended in 80% formamide loading buffer (a solution of 80% v/v formamide, 1 mM EDTA, 0.1% xylene cyanol, and 0.1% bromophenol blue). All reactions, along with Maxam−Gilbert G+A and C+T sequencing reactions,[21] were heat-denatured at 90 °C for 3 min and quickly chilled on ice. The samples (1−2 μL, $(2-5) \times 10^3$ cpm) were loaded onto 12% polyacrylamide/7 M urea sequencing gels, electrophoresed at 1900 V for approximately 2 h,[22] transferred to a cassette, and stored at −80 °C with Fuji X-ray film (RX-U). The gels were analyzed by autoradiography with a densitometer and Bio-Rad Molecular Analyst software (version 2.1). The intensities of the spots resulting from piperidine treatment were determined by volume integration.

(17) (a) Melvin, T.; Plumb, M. A.; Botchway, S. W.; O'Neill, P.; Parker, A. W. *Photochem. Photobiol.* **1995**, *61*, 584. (b) Spassky, A.; Angelov, D. *Biochemistry* **1997**, *36*, 6571.

(18) (a) Patterson, S. E.; Coxon, J. M. Strekowski, L. *Bioorg. Med. Chem.* **1997**, *5*, 277. (b) Hutter, M.; Clark, T. *J. Am. Chem. Soc*. **1996**, *118*, 7574. (c) Colson, A.-O.; Besler, B.; Close, D. M.; Sevilla, M. D. *J. Phys. Chem.* **1992**, *96*, 661. (d) Sponer, J.; Leszczynski, J.; Hobza, P. *J. Phys. Chem.* **1996**, *100*, 5590. (e) Part, F.; Houk, K. N.; Foote, C. S. *J. Am. Chem. Soc*. **1998**, *120*, 845.

(19) (a) Maxam, A. M.; Gilbert, W. *Proc. Natl. Acad. Sci. U.S.A.* **1977**, *74*, 560. (b) Maniatis, T.; Fritsch, E. F.; Sambrook, J. *Molecular Cloning*; Cold Spring Harbor Laboratory Press: Plainview, NY, 1982.

(20) Sambrook, J.; Fritsch, E. F.; Maniatis, T. *Molecular Cloning: A laboratory Manual*, 2nd ed.; Cold Spring Harbor Laboratory Press: Plainview, NY, 1989.

(21) Maxam, A. M.; Gilbert, W. In *Methods in Enzymology*; Grossman, L., Moldave, K., Eds.; Academic Press: New York, 1980; Vol. 65, p 499.

(22) (a) Rickwood, D.; Hames, B. D. *Gel Electrophoresis of Nucleic Acids: A Practical Approach*, 2nd ed.; IRL Press: New York, 1990. (b) Brown, T. A. *DNA Sequencing: The Basics;* IRL Press: New York, 1994.

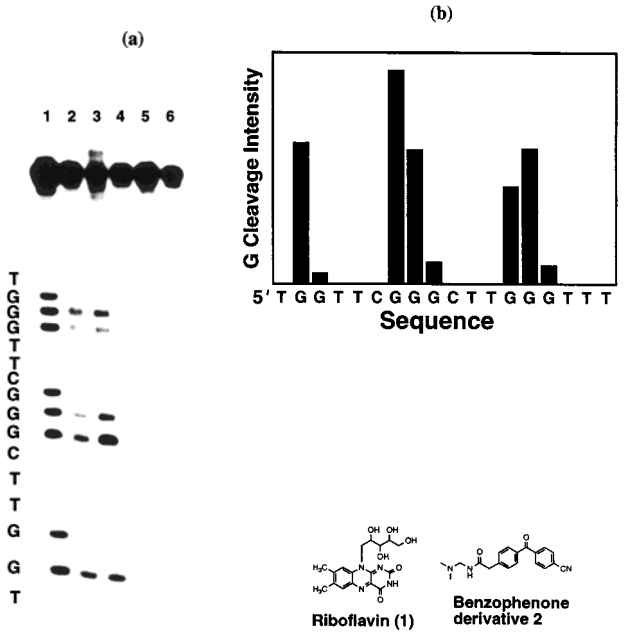

Figure 1. (a) Autoradiograms of a denaturing gel electrophoresis for 5′-^{32}P-end-labeled ODN 5′-CGTACTCTTGGTTCGGGCTTGGGTTTCTTTCTT-3′ sequence after photooxidation of the duplex in the presence of photosensitizers, riboflavin (**1**) and benzophenone derivative **2**. The 5′-^{32}P-end-labeled ODN duplex containing a photosensitizer and calf thymus DNA was irradiated with a transilluminator under the conditions described in the Experimental Section. (Lane 1) Maxam−Gilbert sequencing reactions G+A; (lane 2) irradiated DNA in the presence of **1** (45 μM, 366 nm, 40 min); (lane 3) irradiated DNA in the presence of **2** (50 μM, 312 nm, 40 min); (lane 4) irradiated DNA without sensitizer (366 nm, 30 min); (lane 5) irradiated DNA without sensitizer (312 nm, 40 min); (lane 6) DNA, dark control, no piperidine treatment. (b) The histogram representing relative intensities of cleavage bands obtained by densitometric assay of lane 3 (benzophenone derivative **2** sensitization).

Experimental Results

5′-^{32}P-End-labeled ODN 33 mer, which includes simultaneously two triplet sequences of 5′-TGGGT-3′ and 5′-CGGGC-3′ and one doublet sequence of 5′-TGGT-3′, was hybridized to the complementary strand in an aerated buffer of sodium cacodylate. In the presence of photosensitizer such as riboflavin (**1**)[1g,12] and cyano-substituted benzophenone **2**,[13a] the 5′-^{32}P-end-labeled ODN duplex was photoirradiated under the conditions shown in Figure 1. After hot piperidine treatment, the mixture was analyzed by gel electrophoresis. Figure 1a shows the autoradiogram, whereas Figure 1b illustrates the selectivity for the damage on two GGG triplets and a GG doublet induced by photoirradiated riboflavin.

It can be easily seen from Figure 1 that the guanine base is selectively damaged. The observed selectivities for TG_1G_2T ($G_1 \gg G_2$), $TG_1G_2G_3T$ ($G_2 > G_1$), and $CG_1G_2G_3C$ ($G_1 > G_2$) are consistent with the previously reported results for GGG triplets. It was also confirmed that such selectivity is not altered by the photosensitizer used. In agreement with previously observed selectivity,[1b−d] 5′-$CG_1G_2G_3C$-3′ is a unique sequence that exhibits high G_1 selectivity, in contrast to the G_2 selectivity observed for other GGG triplets, such as $AG_1G_2G_3T$, $TG_1G_2G_3T$, and $AG_1G_2G_3A$.[12a,14] In all cases, the 3′-G (G_3) was far less reactive than G_1 and G_2. Since there is a possibility that such unique selectivity observed for 5′-$CG_1G_2G_3C$-3′ arises from the difference in the duplex structure, such as A-form rather than normal B-form, we measured the CD spectra of the duplex oligomers, 5′-CATTCGGGCTTG-3′/5′-CAAGCCCGAATG-3′ and 5′-ATGGGTACCCAT-3′ (self-complementary). As shown in Figure 2, both duplexes gave typical CD spectra of B-form DNA, implying that the selectivity of 5′-$CG_1G_2G_3C$-3′ may arise from the intrinsic chemical property of this sequence.

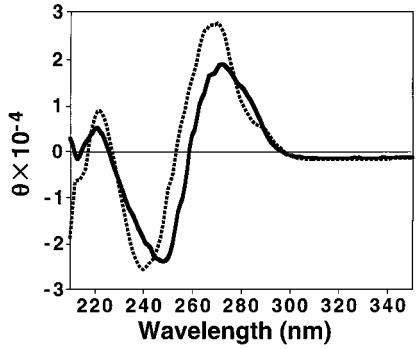

Figure 2. CD spectra of 5′-CATTCGGGCTTG-3′/5′-CAAGCCGAATG-3′ (solid line) and 5′-ATGGGTACCCAT-3′ (self-complementary, dotted line) (150 mM, base concentration) in 10 mM sodium cacodylate buffer, NaCl 100 mM (pH = 7.0) at 4 °C.

Calculational Details. We performed ab initio molecular orbital calculations to elucidate the selectivities of 5′-TGGG-3′ and 5′-CGGG-3′ sequences toward one-electron oxidation. The geometries of 5′-TGGG-3′ and 5′-CGGG-3′ sequences possessing double-stranded B-form structure were constructed using the Insight II program with standard B-form geometrical parameters which have been optimized by X-ray crystallographic analysis of relevant monomers and X-ray diffraction data of polymers.[23] All the sugar backbones of the duplex 4 mer were replaced by methyl groups, keeping the position of all atoms fixed. For the calculations of radical cations and deprotonated neutral radicals of the 5′-TGGG-3′ and 5′-CGGG-3′ sequences, the same geometries constructed by the above procedure were employed without geometry optimization. The charge densities and spin densities are summed for every base of the GGG triplet to distinguish which of the guanines has localized positive charge and spin densities corresponding to the states of the radical cation and neutral radical.

All calculations were carried out at the HF/6-31G level using the Gaussian 94 program package.[24] In our previous paper, we demonstrated that the Koopmans' IPs estimated at the HF/6-31G* level with polarization function are useful for predicting the relative reactivity toward one-electron oxidation of G-containing 5′-TXGYT-3′.[3] The analysis of HOMO is also very important for GG and GGG sequences. Koopmans' IP is equal to the HOMO energy with switched sign, while the vertical IP is defined by the difference in energies between the neutral ground state and the radical cation state in which the one electron is removed from the ground state. Therefore, the vertical IP depends on the calculational accuracy of the radical cation state.

To confirm the effects of polarization function, the Koopmans' and vertical IPs of GGG triplets were evaluated with and without the polarization functions. As can be seen from Table 1, the 6-31G* basis set gave Koopmans' IPs of 6.42 and 7.06 eV for the double and single strands of GGG triplets, respec-

(23) (a)Arnott, S.; Hukins, D. W. L. *Biochem. Biophys. Res. Commun.* **1972**, *47*, 1504. (b) Arnott, S.; Selsing, E. *J. Mol. Biol*. **1974**, *88*, 509.

(24) Frisch, M. J.; Trucks, G. W.; Schlegel, H. B.; Gill, P. M. W.; Johnson, B. G.; Robb, M. A.; Cheeseman, J. R.; Keith, T. A.; Petersson, G. A.; Montgomery, J. A.; Raghavachari, K.; Al-Laham, M. A.; Zakrzewski, V. G.; Oritiz, J. V.; Foresman, J. B.; Cioslowski, J.; Stefanov, B. B.; Nanayakkara, A.; Challacombe, M.; Peng, C. Y.; Ayala, P. Y.; Chen, W.; Wong, M. W.; Andres, J. L.; Replogle, E. S.; Gomperts, R.; Martin, R. L.; Fox, D. J.; Binkley, J. S.; Defrees, D. J.; Baker, J.; Stewart, J. P.; Head-Gordon, M.; Gonzalez, C.; Pople, J. A. *Gaussian 94*; Gaussian, Inc.: Pittsburgh, PA, 1995.

Table 1. Ionization Potentials (eV) of Stacked Base-Paired Oligodeoxynucleotides Calculated at the HF/6-31G Level

base	Koopmans' IP	vertical IP
TGGG	6.45	4.98 ($TG^{+\bullet}GG$)
		5.03 ($TGG^{+\bullet}G$)
		7.44 ($ACC^{+\bullet}C$[a])
CGGG	6.39	5.02 ($CGG^{+\bullet}G$)
GGG	6.58 (6.42)[b]	5.18 (4.98)[b]
GGG[c]	7.34 (7.06)[b]	5.88 (5.61)[b]

[a] Complementary strand of TGGG. [b] Estimation at HF/6-31G* level. [c] Single strand.

tively, while the 6-31G basis set without polarization function also gave 6.58 and 7.34 eV. As the vertical IPs, the 6-31G* gave 4.98 and 5.61 eV and the 6-31G gave 5.18 and 5.88 eV for the double and single strands, respectively. Although the effects of the polarization functions are slightly larger than 0.2 eV for the single strand, they are less than 0.2 eV for the double strand. This examination shows that the 6-31G basis set is available for studying the stabilities of neutral, radical cation, and neutral radical states.

Theoretical Analyses on Radical Cations of 5′-TGGG-3′ and 5′-CGGG-3′. Table 1 summarizes the Koopmans' IPs of 5′-TGGG-3′ and 5′-CGGG-3′ sequences. The IPs of both 5′-TGGG-3′ and 5′-CGGG-3′ sequences are almost the same, with a difference of only 0.06 eV. The IP of 6.42 eV of double-stranded GGG shown in Table 1 is smaller than that (6.73 eV)[9b] of (GG)/(CC) estimated previously at the HF/6-31G* level, indicating that the addition of guanine base to GG doublet considerably decreases the ionization potential, in agreement with the previous report by Houk and Foote.[18e] Addition of thymine and cytosine at the 5′-side also induced an additional decrease of IP from 6.58 eV to 6.45 and 6.39 eV, respectively. These estimations mean that both sequences of TGGG and CGGG can act as thermodynamic sinks in hole migration through DNA π stack. It is therefore reasonable to consider that the cation radical states of 5′-TGGG-3′ and 5′-CGGG-3′ sequences are the first step of one-electron oxidation.

For the radical cations of XGGG (X = T and C), three possible states, $XG^{+\bullet}GG$, $XGG^{+\bullet}G$, and $XGGG^{+\bullet}$, are to be considered. The hole is expected to migrate reversibly among these radical cation states.[2,25] To elucidate the stabilities of the radical cations of both 5′-TGGG-3′ and 5′-CGGG-3′ sequences, we performed SCF calculations of three states of the radical cations. In the case of the 5′-TGGG-3′ sequence, the first SCF calculation is automatically converged to the state of 5′-$TGG^{+\bullet}G$-3′. We tried calculations again to find the states of 5′-$TG^{+\bullet}GG$-3′ and 5′-$TGGG^{+\bullet}$-3′ by constructing the corresponding initial guesses of the SCF calculations by changing the occupation number of electrons of the molecular orbitals of the 5′-$TGG^{+\bullet}G$-3′ state. The expected 5′-$TG^{+\bullet}GG$-3′ state was obtained, but 5′-$TGGG^{+\bullet}$-3′ was not found, as shown in Table 2. Although similar procedures were carried out for the 5′-CGGG-3′ sequence, only the 5′-$CGG^{+\bullet}G$-3′ state was found.

It can be seen from Table 2 that the 5′-$TG_1{}^{+\bullet}G_2G_3$-3′ state is more stable than the 5′-$TG_1G_2{}^{+\bullet}G_3$-3′ state but only by 1.3 kcal/mol, showing that they are considered to be isoenergetic states. The hole may be trapped by G_1 and G_2 with an equal probability in the radical cations of 5′-TGGG, and the hole can reversibly move between 5′-$TG^{+\bullet}GG$-3′ and 5′-$TGG^{+\bullet}G$-3′. However, these results conflict with the experimentally observed high G_2 selectivity for 5′-$TG_1G_2G_3$-3′.

(25) Jortner, J.; Bixon, M.; Langenbacher, T.; Michel-Beyerle, M. E. *Proc. Natl. Acad. Sci. U.S.A.* **1998**, *95*, 12759.

Table 2. Relative Stabilities (kcal/mol) of Radical Cations and Neutral Radicals of 5′-TGGG-3′ and 5′-CGGG-3′ at the HF/6-31G Level

base pairs, E_{rel}	XG*GG[a]	XGG*G[a]	XGGG*[a]
	5′-TGGG-3′ Base Pair		
radical cations	$TG^{+\bullet}GG$	$TGG^{+\bullet}G$	$TGGG^{+\bullet}$
E_{rel}	0.0[b]	1.3	not found
neutral radicals	$TG^{\bullet}GG$	$TGG^{\bullet}G$	$TGGG^{\bullet}$
E_{rel}	2.4	0.0[c]	9.1
	5′-CGGG-3′ Base Pair		
radical cations	$CG^{+\bullet}GG$	$CGG^{+\bullet}G$	$CGGG^{+\bullet}$
E_{rel}	not found	found[d]	not found
neutral radicals	$CG^{\bullet}GG$	$CGG^{\bullet}G$	$CGGG^{\bullet}$
E_{rel}	7.8	0.0[e]	not found

[a] The asterisk means radical cation (+•) or radical (•). [b] Total energy is −4022.32099 au. [c] Total energy is −4021.83214 au. [d] Total energy is −4038.32504 au. [e] Total energy is −4037.83535 au.

Table 3. Orbital Energies (au) Corresponding to the Radical Orbital (SOMO) and HOMO

	radical orbital	HOMO
TGGG		−0.23696
$TG^{+\bullet}GG$	−0.44973	−0.32780
$TGG^{+\bullet}G$	−0.44798	−0.34437
$TGG^{\bullet}G$	−0.29186	−0.25137
$TG^{\bullet}GG$	−0.28754	−0.24286
$TGGG^{\bullet}$	−0.32064	−0.24353
CGGG		−0.23475
$CGG^{+\bullet}G$	−0.44725	−0.32288
$CGG^{\bullet}G$	−0.29256	−0.24870
$CG^{\bullet}GG$	−0.30267	−0.24325

On the other hand, in the case of the 5′-$CG_1G_2G_3$-3′ sequence, theoretical calculations show that the hole may be trapped only at G_2, as indicated in Table 2. The hole, if generated at G_1 of the largest HOMO, will rapidly pass through the radical cation state 5′-$CG^{+\bullet}GG$-3′ to reach to 5′-$CGG^{+\bullet}G$-3′. However, as a next pathway from 5′-$CG^{+\bullet}GG$-3′, there are at least two possibilities: (i) the hole migrates to adjacent G_2 to yield the stable 5′-$CG_1G_2{}^{+\bullet}G_3$-3′ state and (ii) the deprotonation from G_1 occurs to produce the corresponding neutral radical 5′-$CG_1{}^{\bullet}G_2G_3$-3′. In fact, the 5′-$CG_1{}^{\bullet}G_2G_3$-3′ state is theoretically obtained as described in next section (see also Table 2). These two pathways of hole migration and deprotonation are considered to be competitive in one-electron oxidation reaction. Therefore, the theoretical calculations indicate that the experimentally observed selectivity of 5′-CGGG is expected to be caused from the stability and/or the unique electronic structure of deprotonated neutral radical state (5′-CGGG)•, not the stability of $(5'\text{-CGGG})^{+\bullet}$ radical cation states.

It is easily seen from Table 1 that the vertical IPs of both 5′-TGGG-3′ (4.98 eV) and 5′-CGGG-3′ (5.02 eV) sequences are very close, being insensitive to which base is stacked at the 5′-side. However, when compared with double-stranded simple GGG, the thymine and cytosine at the 5′-side cause an additional decrease of the vertical IPs. These effects are also found for the Koopmans' IPs.

Table 3 summarizes the orbital energies of the HOMO and the singly occupied MO (SOMO) corresponding to the radical orbitals. From Table 3, the radical orbitals of the 5′-$TG^{+\bullet}GG$-3′, 5′-$TGG^{+\bullet}G$-3′, and 5′-$CGG^{+\bullet}G$-3′ states do not apparently coincide with their HOMOs. The radical orbitals are largely stabilized compared with the HOMOs, which correspond to the 304th α MO in both the 5′-TGGG-3′ and 5′-CGGG-3′ sequences. For example, the radical orbitals are corresponding to the 291st, 292nd, and 291st α MO in the 5′-$TG^{+\bullet}GG$-3′, 5′-$TGG^{+\bullet}G$-3′, and 5′-$CGG^{+\bullet}G$-3′ states, respectively. The dis-

agreement between the SOMO and HOMO is not unusual. Each orbital is localized on each base in the radical cation system. The SOMO radical orbital, which is localized on the positively charged guanine base, is largely stabilized due to the net positive charge and apparently corresponds to the HOMO of $G^{+\bullet}$ in the 5′-TG$^{+\bullet}$GG-3′, 5′-TGG$^{+\bullet}$G-3′, and 5′-CGG$^{+\bullet}$G-3′ states. Therefore, the HOMOs of the 5′-TG$^{+\bullet}$GG-3′, 5′-TGG$^{+\bullet}$G-3′, and 5′-CGG$^{+\bullet}$G-3′ states comes from the HOMOs of other bases, except for $G^{+\bullet}$ in TGGG and CGGG sequences. This considerable energy-lowering of the radical orbitals of the radical cation $G^{+\bullet}$ is in harmony with the hopping mechanism of hole migration via guanine radical cation proposed theoretically[25] and experimentally.[2a] The HOMOs of the 5′-TG$^{+\bullet}$GG-3′ and 5′-TGG$^{+\bullet}$G-3′ states are localized on G* bases of (TGGG*)/(CCCA) and (TG*GG)/(CCCA), respectively, while the 5′-CGG$^{+\bullet}$G-3′ state is on the G* base of (CGGG)/(CCCG*).

Theoretical Analyses on Neutral Radicals of 5′-TGGG-3′ and 5′-CGGG-3′. When the radical cation of guanine is formed in a double-stranded structure, the N1 proton immediately transfers to N3 of cytosine of the base pair with pK_a = 4.3.[5] The $G^{+\bullet}$ is a strong acid with pK_a = 3.9,[26] which can easily generate the neutral radical through deprotonation after one-electron oxidation in neutral pH. In fact, ESR studies have shown that the N1 proton is the one to be lost in this process.[27] The proton is expected to be released into the solvent under our experimental condition of neutral pH.

For the 5′-TGGG-3′ sequence, three neutral radical states of 5′-TG$^{\bullet}$GG-3′, 5′-TGG$^{\bullet}$G-3′, and 5′-TGGG$^{\bullet}$-3′, which are deprotonated states from N1 of guanine, were obtained by the SCF procedures starting from the initial guess corresponding to the electronic configurations of the three radical states. It is apparent from Table 2 that 5′-TGG$^{\bullet}$G-3′ is the most stable among neutral radical states of 5′-TGGG-3′. The 5′-TGGG$^{\bullet}$-3′ state is less stable by 9.1 kcal/mol than the 5′-TGG$^{\bullet}$G-3′, and the 5′-TG$^{\bullet}$GG-3′ is only 2.4 kcal/mol higher than the 5′-TGG$^{\bullet}$G-3′. These results for the stabilities of three radical states are in good agreement with the experimental observation that G_2 of 5′-$TG_1G_2G_3$-3′ is the most reactive site in DNA one-electron oxidation. As discussed latter, the reactivities of 5′-TG$^{\bullet}$GG-3′ and 5′-TGG$^{\bullet}$G-3′ toward molecular oxygen are expected to be very similar by the analyses of the radical orbitals (SOMOs) of both neutral radical states. Therefore, it can be considered that the selectivity of the 5′-TGGG-3′ sequence is primarily determined by the stability of neutral radical states produced through the radical cations by one-electron oxidation.

From Table 3, the HOMOs of the 5′-TGGG-3′ radical states are apparently not corresponding to the radical orbitals (SOMOs). The HOMOs and SOMOs are destabilized by the deprotonation, and the orbital energies of SOMOs are closer to those of HOMOs than in the cases of radical cations. The HOMO of the 5′-TG$^{\bullet}$GG-3′ state is localized on G* of (TGG*G)/(CCCA), while those of the 5′-TGG$^{\bullet}$G-3′ and 5′-TGGG$^{\bullet}$-3′ are on G* of (TG*GG)/(CCCA).

On the other hand, although only one state of radical cation for the 5′-CGGG-3′ sequence was found, two radical states of 5′-CG$^{\bullet}$GG-3′ and 5′-CGG$^{\bullet}$G-3′ were found, as shown in Table 2. The remaining radical state of 5′-CGGG$^{\bullet}$-3′ was not still found. The 5′-CG$^{\bullet}$GG-3′ state is less stable by 7.8 kcal/mol than the 5′-CGG$^{\bullet}$G-3′ state. This result is not in agreement with the selectivity observed experimentally in DNA photocleavage, where G_1 is more easily damaged than G_2, indicating that, unlike 5′-TGGG-3′, the selectivity of 5′-CG$^{\bullet}$GG-3′ sequence in DNA one-electron oxidation is not determined primarily by the stabilities of radical cations and neutral radicals.

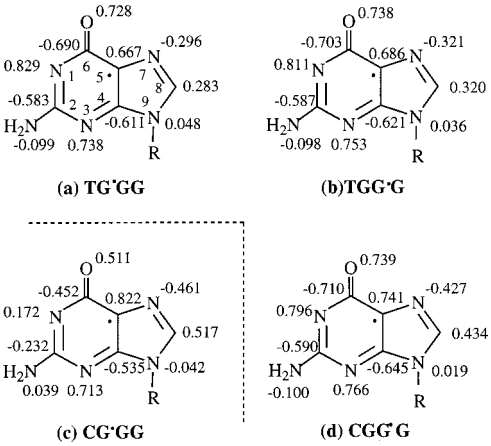

Figure 3. Atomic spin densities of the G$^{\bullet}$ radical in the neutral radical states of (a) 5′-TG$^{\bullet}$GG-3′, (b) 5′-TGG$^{\bullet}$G-3′, (c) 5′-CG$^{\bullet}$GG-3′, and (d) 5′-CGG$^{\bullet}$G-3′.

Scheme 1. Proposed Mechanism of One-Electron Oxidation of Guanine To Give Imidazolone Product **dIz**

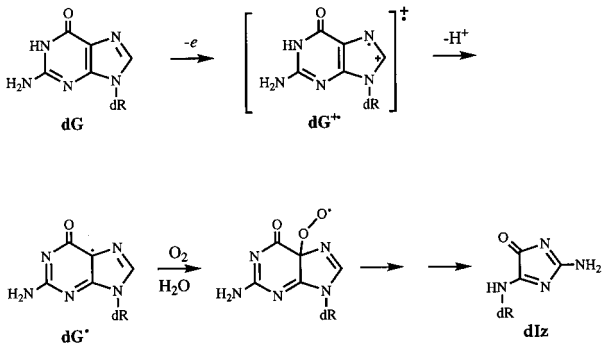

It is also seen from Table 3 that the radical orbitals (SOMOs) of 5′-CG$^{\bullet}$GG-3′ and 5′-CGG$^{\bullet}$G-3′ still do not coincide with the HOMOs. The SOMOs and HOMOs are highly destabilized due to the deprotonation of the corresponding radical cations. Compared with those of the radical cations, the change of orbital energies means that the radical orbitals of the neutral radical states are more reactive than those of the radical cation states. The HOMO of the 5′-CG$^{\bullet}$GG-3′ state is localized on G* of (CGG*G)/(CCCG), while that of the 5′-CGG$^{\bullet}$G-3′ state is on G* of (CG*GG)/(CCCG).

Analyses of Radical Orbitals in Neutral Radical States of 5′-TGGG-3′ and 5′-CGGG-3′. The reaction mechanism of one-electron oxidation of guanine base has been proposed as shown in Scheme 1.[12b,28] The neutral radical **dG$^{\bullet}$** is an important intermediate for the reaction with molecular oxygen to yield ultimately imidazolone product (**dIz**).[12b] Therefore, the reactivity of the neutral guanine radicals generated in the double-stranded B-form DNA was investigated in more detail in order to elucidate the selectivity of 5′-TGGG-3′ and 5′-CGGG-3′ as well as their stabilities.

Before analyzing radical orbitals in neutral radical states, it is interesting to explore the atomic spin densities of guanine radicals in neutral radical states of the 5′-TGGG-3′ and 5′-CGGG-3′ sequences. Figure 3 depicts the atomic spin densities of G$^{\bullet}$ radical of four neutral radical states of the 5′-TGGG-3′ and 5′-CGGG-3′ sequences. The C5's of all states

(26) Candeias, L. P.; Steenken, S. *J. Am. Chem. Soc*. **1989**, *111*, 1094.
(27) Hildebrand, K.; Schulte-Frohlinde, D. *Free Radical Res. Commun*. **1990**, *11*, 195.
(28) (a) Cadet, J.; Berger, M.; Buchko, C. W.; Joshi, P. C.; Raoul, S.; Ravana, J.-L. *J. Am. Chem. Soc*. **1994**, *116*, 7403. (b) Viala, C.; Pratviel, G.; Claparols, C.; Meunier, B. *J. Am. Chem. Soc*. **1998**, *120*, 11548.

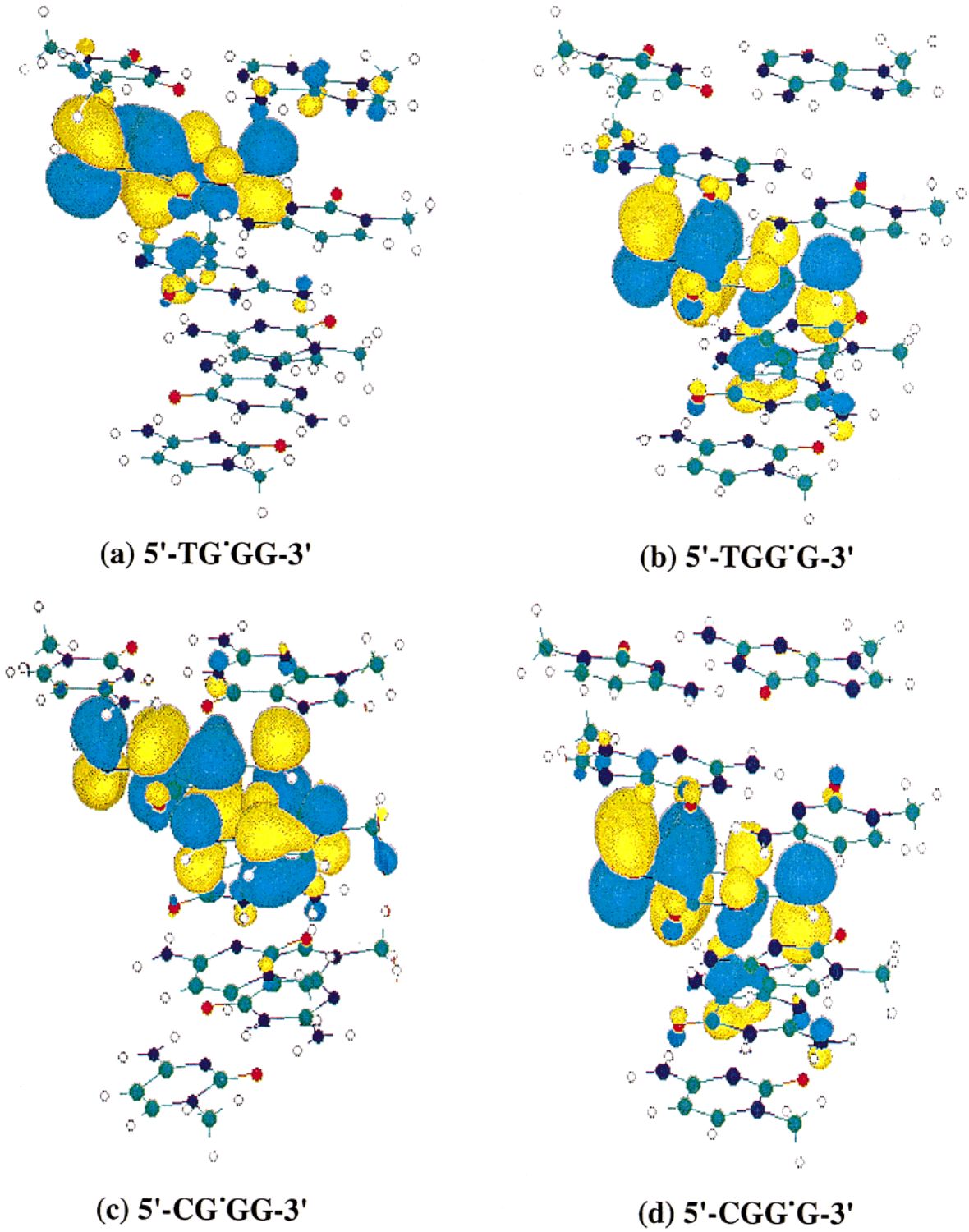

Figure 4. Three-dimensional views of the radical orbitals of 5′-TGGG-3′ and 5′-CGGG-3′ neutral radicals. Each radical orbital is viewed from the same direction that the C6−N1 bond in the G• radical guanine is faced to the front. The green rigid circle corresponds to the carbon atom, red the oxygen atom, and blue the nitrogen atom. The white circle indicates hydrogen atom. (a) 5′-TG•GG-3′, (b) 5′-TGG•G-3′, (c) 5′-CG•GG-3′, and (d) 5′-CGG•G-3′.

have relatively large spin densities from 0.667 to 0.822, in agreement with the proposed oxidation mechanism of guanine radical under aerobic conditions; i.e., molecular oxygen preferentially attacks on C5 of guanine neutral radical to yield ultimately imidazolone product (**dIz**) via C5 hydroperoxy intermediate (Scheme 1).[5,12b,28,29] The spin densities on C5s of 5′-TG•GG-3′ (a) and of 5′-TGG•G-3′ (b) are nearly equal, while those of 5′-CG•GG-3′ (c) and 5′-CGG•G-3′ (d) are different by 0.08; i.e., the spin density of C5 of 5′-CG•GG-3′ (c) is much larger than that of 5′-CGG•G-3′ (d). It can be easily seen from Figure 3 that the patterns of spin densities are classified into two different groups. One group is a set of 5′-TG•GG-3′ (a), 5′-TGG•G-3′ (b), and 5′-CGG•G-3′ (d) radical states, and the other is 5′-CG•GG-3′ (c). The spin densities on deprotonated

(29) Bernstein, R.; Part, F.; Foote, C. S. *J. Am. Chem. Soc*. **1999**, *121*, 464.

N1, C2, and C6 are remarkably different between these two groups. The N1 atoms in the former group have large spin densities from 0.796 to 0.829, while the latter has a small value of only 0.172. C6 in 5′-CG•GG-3′ (c) has a smaller negative spin density of −0.452, compared with ca. −0.7 for the former group. Further, C2 of 5′-CG•GG-3′ (c) has only half value of the corresponding atoms in the former group. However, the summations of atomic spin densities of G• radicals in both groups are nearly equal to unity, even if the spin densities on each atom are remarkably different from each other. These results apparently suggest that the electronic structures of the G• radicals are quite different between these two groups, indicating that G• radicals of both groups are expected to be located under a different interaction circumstance induced by base stacking and base pairing in the B-form DNA.

Although the atomic spin densities correspond to the summation of contributions from all occupied MOs, it is also important to observe carefully the radical orbitals (SOMOs) which are responsible for the reactivity of the oxidation reaction. Figure 4 depicts the molecular orbitals corresponding to the radical orbitals in 5′-TG•GG-3′ (a), 5′-TGG•G-3′ (b), 5′-CG•GG-3′ (c), and 5′-CGG•G-3′ (d) neutral radicals. It can be seen from Figure 4 that, in all cases, the radical orbitals are π-type orbitals which are spread over the guanine base. The radical orbital of the 5′-CGG•G-3′ (d) state has entirely the same shape (for example, the magnitude of robe and phase relationship) as that of 5′-TGG•G-3′ (b) and slightly interacts with the imidazole ring of the guanine at the 3′-side. In addition, the radical orbital of 5′-TG•GG-3′ (a) is also quite similar to the one discussed above and interacts slightly with the imidazole ring of the 3′-side guanine. In fact, the phase relationships of the radical orbitals in both cases totally coincide with each other. On the other hand, it is easily found from Figure 4 that the radical orbital of the 5′-CG•GG-3′ (c) state is drastically different from the three radicals discussed above, being largely delocalized on the guanine base and on the paired cytosine base as well, although it also interacts slightly with the pyrimidine ring of the 3′-side guanine. These behaviors in the radical orbitals are in agreement with those of the atomic spin densities of the guanine radical discussed above.

It is conceivable from the similarity of the radical orbitals of G_1• and G_2• in the 5′-$TG_1G_2G_3$-3′ neutral radical shown in Figure 4 that the reactivity of G_1• and G_2• radicals toward molecular oxygen might be very similar, with almost equal activation energy. It seems not unlikely that the base-paired 5′-TG_1•G_2G_3-3′ radical would be converted reversibly to the 5′-TG_1G_2•G_3-3′ radical via the radical cations (5′-TGGG-3′)•+, although there is no direct path between the two radical states. However, under the condition of neutral pH, the neutral radical states, (5′-TGGG-3′)•, are preferentially generated from the radical cations, (5′-TGGG-3′)•+, as shown in Figure 5. Therefore, the selectivity of the reaction in the 5′-$TG_1G_2G_3$-3′ sequence may be determined primarily by the difference of the stability between 5′-TG_1•G_2G_3-3′ and 5′-TG_1G_2•G_3-3′ states as discussed above.

On the other hand, as shown in Figure 4c, G_1• in the 5′-CG_1•G_2G_3-3′ state apparently exists in a unique interacting environment which is induced by strong stacking interaction with the 5′-side guanine of the opposite strand, unlike G_1• in the 5′-TG_1•G_2G_3-3′ state. On the contrary, G_2• of the 5′-CG_1G_2•G_3-3′ state exists in an interacting environment very similar to that of G_2• of the 5′-TG_1G_2•G_3-3′ state. This dramatic discrepancy seems to be the origin of the selectivity between G_1 and G_2; i.e., G_1 is more reactive than G_2 in one-electron oxidation of the 5′-$CG_1G_2G_3$-3′ sequence.

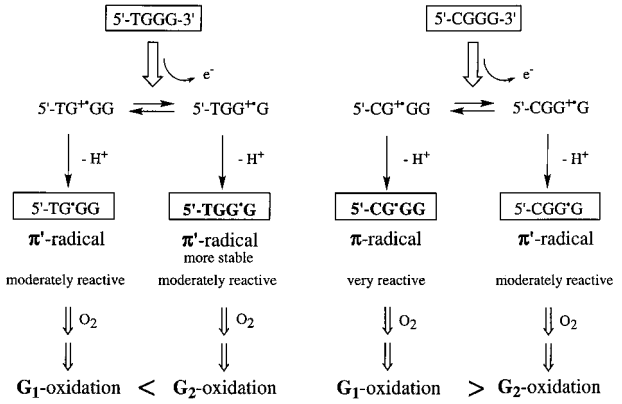

Figure 5. Schematic representation of reaction pathways of 5′-TGGG-3′ and 5′-CGGG-3′ by one-electron oxidation.

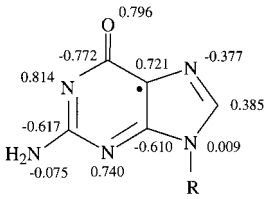

Figure 6. Spin densities of deprotonated neutral guanine radical in monomer at HF/6-31G level.

While molecular oxygen is considered to attack on C5 of the guanine neutral radical as shown in Scheme 1,[5,28,29] the spin density on the C5 positions of the 5′-CG_1•G_2G_3-3′ state is much larger than that of the 5′-CG_1G_2•G_3-3′ state, as shown in Figure 4. The high reactivity of the 5′-CG_1•G_2G_3-3′ state cannot be solely explained by superdelocalizability derived from the frontier electron theory for the corresponding radical orbital, and another explanation is apparently necessary. Probably, the reaction of the G_1• radical orbital with molecular oxygen may proceed with a smaller activation energy compared with that of the G_2• radical orbital. The transition state for the oxygen adduct formation ultimately leading to imidazolone product (**dIz**) should be explicitly found to elucidate the discrepancy of the reactivity between the 5′-CG•GG-3′ and 5′-CGG•G-3′ states.

Figure 6 shows theoretical values of the atomic spin densities for the deprotonated neutral guanine radical in monomer. The atomic spin densities shown in Figure 6 are very similar to those of the 5′-CGG•G-3′ (d) and 5′-TGGG-3′ radicals (a and b) shown in Figure 3, indicating that the electronic structures of G• radicals in the 5′-CGG•G-3′ and (5′-TGGG-3′)• radicals behave very similarly to monomer G•, even in the DNA duplex. On the contrary, it is apparent that G_1• radical in the 5′-CG_1•G_2G_3-3′ state exists in a unique interacting environment compared with other G• radicals, as depicted in Figure 4c. It is therefore concluded that the unique and high reactivity of G_1• of 5′-CG_1•G_2G_3-3′ is induced by the strong stacking interaction with the 5′-side G of the opposite strand.

Summary and Concluding Remarks. The selectivites for photoinduced one-electron oxidation of 5′-TGGG-3′ and 5′-CGGG-3′ have been examined experimentally and by ab initio MO calculations. Figure 5 summarizes the selectivites of the initial stages of one-electron oxidation of both the 5′-TGGG-3′ and 5′-CGGG-3′ sequences.

Our conclusions are summarized as follows:

(1) Although all 5′-G_1G_2-3′ sequences in B-form DNA have high G_1 selectivity for one-electron oxidation, 5′-$G_1G_2G_3$-3′ triplets have G_2 selectivity in the cases of 5′-$TG_1G_2G_3$T-3′ and 5′-$AG_1G_2G_3$A-3′ sequences. The spin densities of G_1• and G_2•

have similar patterns, and the shapes of the radical orbitals are also similar. The selectivity is primarily due to the stability of the (5′-$G_1G_2G_3$-3′)• neutral radicals; that is, the 5′-G_1G_2•G_3-3′ is more stable in energy than the 5′-G_1•G_2G_3-3′. The large spin densities on C5's of 5′-TG_1•G_2 G_3-3′ and 5′-TG_1G_2•G_3-3′ are also consistent with the fact that molecular oxygen attacks preferentially on this position to give imidazolone product (**dIz**).

(2) The 5′-$CG_1G_2G_3$-3′ sequence is unique, with high G_1 selectivity. The spin density on N1 of G_1• is distinguishably different from the corresponding spin density of G_2•, which has a pattern similar to those of G_1• and G_2• in 5′-$TG_1G_2G_3$-3′ triplets. While the radical orbital (SOMO) of G_1• is delocalized up to the paired cytosine base, the radical orbital of G_2• is essentially localized on guanine base. The unique electron population of 5′-CG_1•G_2G_3-3′ originates from the stacking interaction with the 5′-side G of the opposite strand. This drastic difference in the electron populations in the radical orbitals can explain why G_1 is more reactive than G_2.

(3) The radical orbitals (SOMOs) in states of radical cations and neutral radicals of 5′-TGGG-3′ and 5′-CGGG-3′ are not the highest occupied molecular orbitals (HOMOs). The radical orbitals of the radical cations are more stabilized than those of the radicals.

(4) The selectivity of the oxidation is not determined solely by the stability of radical cations and/or neutral radicals. The electronic structures corresponding to the radical orbitals may play a very important role for the selectivity.

The guanine is most easily oxidized among the nucleobases, and the GGG triplets are most effective. However, as elucidated in this work, the guanine base is drastically affected by the interaction fields induced by base pairing and base stacking. These effects have naturally to be taken into account in order to explain the reactivity and the selectivity in one-electron oxidation of GGG triplets. The electron-loss center created in duplex DNA ultimately moves to end up at the G residue via hole migration through the DNA duplex. It may not be thought as a sole pathway that the hole passes through the stacked bases due to the overlap of π-electrons of the stacked bases.

Acknowledgment. This work was supported by CREST (Core Research for Evolutional Science and Technology) of Japan Science and Technology Corporation (JST).

JA991032T